

# X-ray diffraction microscopy based on refractive optics



T. Roth<sup>\*,1</sup>, C. Detlefs, I. Snigireva, A. Snigirev

European Synchrotron Radiation Facility, B.P. 220, 6 rue Jules Horowitz, 38043 Grenoble Cedex 9, France

## ARTICLE INFO

### Article history:

Received 24 September 2014

Received in revised form

24 November 2014

Accepted 27 November 2014

Available online 1 December 2014

### Keywords:

Diffraction imaging

X-ray microscopy

Compound refractive lenses

X-ray topography

## ABSTRACT

We describe a diffraction microscopy technique based on refractive optics to study structural variations in crystals. The X-ray beam diffracted by a crystal was magnified by Beryllium parabolic refractive lenses on a 2D X-ray camera. The microscopy setup was integrated into the 6-circle Huber diffractometer at the ESRF beamline ID06. Our setup allowed us to visualize structural imperfections with a resolution of  $\approx 1 \mu\text{m}$ . The configuration, however, can easily be adapted for sub- $\mu\text{m}$  resolution.

© 2014 Elsevier B.V. All rights reserved.

## 1. Introduction

X-ray diffraction imaging, known later as X-ray topography, originated in the late 1920s and early 1930s, when researchers revealed the internal structure of individual Laue spots in diffraction patterns [1,2]. To improve the resolution, fine grain photographic emulsions were exposed and examined under optical microscopes – for this reason the technique was sometimes called X-ray microscopy [3]. This method was applied for both mapping of strains in heavily deformed materials such as cold-worked metals and alloys [3] and studies of individual defects in near-perfect single crystals [4].

It was assumed that each point on the film or detector corresponds to a small volume in the reflecting crystal. Simple geometrical optics then requires the incoming X-ray beam to be tightly collimated, and the film to be placed as closely as possible to the sample. The achievable resolution is then limited by the detector resolution, at best 500 nm [5] but more typically 1  $\mu\text{m}$ .

However, in the absence of X-ray optics between the sample and the film diffraction effects progressively blur the image with increasing sample-to-detector distance. For a typical experimental setup (wavelength  $\lambda = 1 \text{ \AA}$ , sample-to-detector distance  $s = 1 \text{ cm}$ , and sample feature size  $d = 1 \mu\text{m}$ ) the diffraction limited resolution due to propagation of the perturbed wavefront from the exit surface of the crystal to the detector can be approximated as

$$\delta \approx \frac{\lambda}{d} \cdot s = \frac{10^{-10} \text{ m}}{10^{-6} \text{ m}} \cdot 10^{-2} \text{ m} = 1 \mu\text{m}. \quad (1)$$

Note that to image  $10 \times$  smaller features on the sample ( $d = 100 \text{ nm}$  and therefore  $\delta = 100 \text{ nm}$ ) the sample-to-detector distance would have to be decreased by a factor of 100,  $s = 100 \mu\text{m}$ . In most cases this is technically not feasible. Furthermore, to the best of our knowledge, 2D imaging detectors with a spatial resolution of 100 nm are not yet available.

On the other hand, conventional X-ray microscopy techniques as proposed by Kirkpatrick and Baez [6,7] have been implemented in the hard X-ray domain rather late. Here, an in-line scheme is used where the beam transmitted through the sample is magnified by X-ray optics such as mirrors [8], Fresnel zone plates [9], Bragg–Fresnel lenses [10], or refractive lenses [11]. Such forward scattering techniques are primarily sensitive to spatial variations of the X-ray index of refraction which depends mostly on the local density of the sample.

In this paper we propose a compact scheme for diffraction microscopy using X-ray refractive lenses between the sample and the detector. The insertion of refractive optics into the diffracted beam allows significant improvements of the resolution, potentially down to below 100 nm (a resolution of 300 nm has been demonstrated using a similar lens in transmission X-ray microscopy [12]). Furthermore, the progressive blurring due to the wavefront propagating from the sample to the detector can be overcome by a lens, thus reestablishing the direct mapping of intensity variations on the detector to the reflectivity variations on the sample. In this case the image resolution can, in principle, reach the limit imposed by dynamical diffraction effects within the crystal.

\* Corresponding author.

E-mail address: [thomas.roth@xfel.eu](mailto:thomas.roth@xfel.eu) (T. Roth).

<sup>1</sup> Now at: European XFEL GmbH, Hamburg, Germany.

Recently, Fresnel zone plates have been used in X-ray reflection microscopy to image monomolecular steps at a solid surface [13] and for scanning X-ray topography of strained silicon oxide structures [14]. CRLs have the advantage that efficient focusing can be achieved at higher photon energies,  $E \gg 10$  keV. Note that standard KB mirrors are not suited for imaging setups, as they do not fulfill the Abbe-sine condition. More complicated multi-mirror setups are however being developed to overcome this limitation in transmission geometry [15].

## 2. Experimental details

Our experiment was carried out at the undulator beamline ID06 of the European Synchrotron Radiation Facility. A cryogenically cooled permanent magnet in-vacuum undulator [16] with a period of 18 mm and a conventional in-air undulator with a period of 32 mm, combined with a liquid nitrogen cooled Si (111) monochromator, delivered photons at an energy of 11 keV. A transfocator located at 38.7 m from the source point (electron beam waist position in the middle between the two undulators) acted as a condenser, i.e. it focused the photons onto the sample at 67.9 m distance from the source, using a combination of paraboloid (2D) compound refractive lenses, CRLs, [11]: one lens with radius of curvature at the apex  $R=1.5$  mm and two lenses with  $R=0.2$  mm, all made out of high-purity Beryllium (Be). The use of the condenser-CRLs improved the optical efficiency of the system (absorption of X-rays in the condenser-CRLs was only about 6%), as it increased the flux on the imaged sample area. The divergence of the photon beam is not altered significantly, as the condenser CRL works almost in a 1:1 magnification geometry. A flux of approximately  $2 \times 10^{12}$  photons/s was incident to the sample. The sample was mounted on a six circle diffractometer. The scattering plane coincided with the horizontal plane.

The detector consisted of a scintillator screen, magnifying optics, and a high resolution CCD-camera. The 9.9  $\mu\text{m}$  thick LAG:Eu scintillator on a 170  $\mu\text{m}$  YAG substrate converted X-rays into visible light, which was projected onto the CCD by the objective lens (Olympus UPLAPO  $\times 10$ , numerical aperture 0.4). The CCD camera (pco SensicamQE) had  $1376 \times 1040$  pixels (px) of size 6.45  $\mu\text{m}/\text{px} \times 6.45 \mu\text{m}/\text{px}$  and 12 bit depth, yielding a field of view on the scintillator of  $887 \times 670 \mu\text{m}^2$  with an effective resolution of 1.3  $\mu\text{m}$ . Each CCD pixel imaged an area of  $0.645 \times 0.645 \mu\text{m}^2$  on the scintillator.

In front of the detector, on the same diffractometer arm, a second set of paraboloid Be CRLs (66 lenses with apex-radius of curvature  $R = 50 \mu\text{m}$ ) was mounted as X-ray objective lens, i.e. to image the diffracted intensity pattern at the sample exit surface onto the detector. These lenses were mounted on translation and rotation stages to align the lens stack, in particular to tune

the sample-to-lens distance to achieve best focusing onto the detector.

The focal length of this lens stack at 11 keV was about 14 cm, so that a  $\approx 4$ -fold magnified image was achieved with the lens center placed about 18 cm downstream of the sample. The effective aperture was about 240  $\mu\text{m}$ , giving a corresponding diffraction limit of 130 nm. The transmission through the lens stack is reduced by the absorption from the thinnest lens part, plus the increased absorption for rays travelling further away from the lens center, resulting in an effective aperture with Gaussian profile [10,11]. The first contribution is easy to calculate and gives an absorption of 18%. Considering the size of the illuminated sample ( $\approx 200$  nm, see below) and approximating the reflected beam as a parallel beam, the total absorption is closer to 50%.

Scaling the effective detector resolution by the magnification factor 4 to  $1.3 \mu\text{m}/4 = 0.33 \mu\text{m}$ , we expected a resolution limit of  $\sqrt{(0.33 \mu\text{m})^2 + (130 \text{ nm})^2} \approx 350$  nm with this set-up.

Two samples were imaged in Bragg geometry. The first sample was a Si (111) wafer upon which a regular stripe pattern of amorphous  $\text{SiO}_2$  has been fabricated by thermal oxidation followed by standard photoresist etching. The  $\text{SiO}_2$  layer was  $z = 1.15 \mu\text{m}$  thick, and was etched to fabricate 2  $\mu\text{m}$  wide windows with a period of 4  $\mu\text{m}$ . The substrate was aligned in the diffractometer to set the oxide stripes parallel to the diffraction plane. In order to record magnified diffraction images of the sample the Bragg (333) reflection of the Si substrate (Bragg angle  $\theta_B = 32.63^\circ$ ) was used (Fig. 1).

The second sample was a linear Bragg-Fresnel lens (BFL) fabricated on a Si (111) substrate (for the fabrication process see [17]). The basic geometrical parameters were an outermost zone width of 0.5  $\mu\text{m}$ , a height of the structure of 4.4  $\mu\text{m}$ , and an aperture of 200  $\mu\text{m}$ . Again, the sample was aligned with the structures parallel to the horizontal scattering plane. Again, the Si (333) ( $\theta_B = 32.63^\circ$ ) reflection was studied.

## 3. Resolution

The homogeneous periodicity of the  $\text{SiO}_2$  line pattern (Fig. 2) was used to calibrate the effective magnification of our configuration. The mask used to produce the pattern had a period of 4  $\mu\text{m}$ , in good agreement with the value, 4.1(1)  $\mu\text{m}$ , obtained by scanning electron microscopy (SEM), see Fig. 2f. Our X-ray image of this structure shows 15 periods over 395(5) px (Fig. 2b). The line spacing on the fluorescence screen of the detector was therefore  $0.645 \mu\text{m}/\text{px} \cdot 395 \text{ px}/15 = 17.0(2) \mu\text{m}$ , yielding a magnification factor of  $17.0 \mu\text{m}/4.1 \mu\text{m} = 4.2(1)$  for the CRL stack and  $4.1 \mu\text{m} \cdot 15/395 \text{ px} = 0.156(4) \mu\text{m}/\text{px}$  for the overall experiment. The resulting field of view on the sample was  $\approx 162 \mu\text{m}/\sin(\theta_B)$  in the horizontal (within the scattering plane) and 215  $\mu\text{m}$  in the vertical direction (perpendicular to the scattering plane).

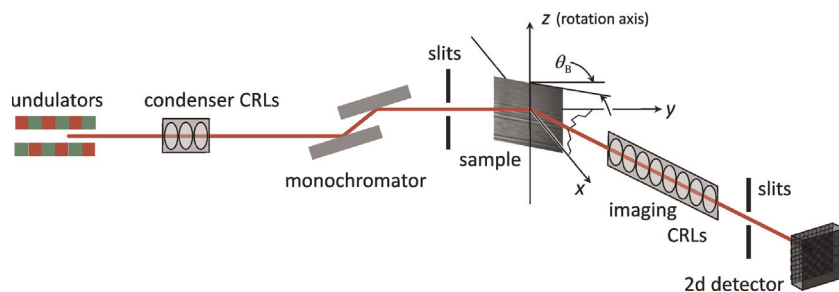


**Fig. 1.** Experimental setup for Bragg diffraction microscopy. 11 keV X-rays impinge on the sample. The diffracted intensity is imaged onto a Sensicam camera via a set of 66 Beryllium compound refractive lenses (CRLs) with an apex-radius of curvature of 50  $\mu\text{m}$ . The scattering plane is horizontal, and the imaged features on the sample were aligned parallel to the scattering plane.

Download English Version:

<https://daneshyari.com/en/article/1534085>

Download Persian Version:

<https://daneshyari.com/article/1534085>

[Daneshyari.com](https://daneshyari.com)